Chance-Constrained Scheduling of Underground Pumped Hydro Energy Storage in Presence of Model Uncertainties

Jean-François Toubeau, *Member, IEEE*, Zacharie De Grève, *Member, IEEE*, Pascal Goderniaux, François Vallée, *Member, IEEE*, and Kenneth Bruninx, *Member, IEEE*

***Abstract*—Abandoned underground quarries or mines may be rehabilitated as natural reservoirs for underground pumped hydro energy storage (UPHES). In addition to the inherent modeling inaccuracies of the traditional PHES that arise from, e.g., approximating the nonlinear pump/turbine head-dependent performance curves, the optimal operation of these underground plants is also affected by endogenous model uncertainties. The latter typically arise from a limited knowledge of the physical characteristics of the system such as the geometry and hydraulic properties of the underground cavity. In this paper, chance-constrained programming is leveraged to immunize the day-ahead scheduling of an UPHES owner against both these model uncertainties and the modeling approximations. The proposed method is tested on a fictitious UPHES system using an existing underground quarry as lower reservoir. Results demonstrate that the methodology allows finding a compromise between conservativeness and economic performance, while being computationally efficient. This model may thus be integrated in the daily scheduling routine of UPHES owners, or may help regulators and system operators to better estimate the available flexibility of such resources.**

***Index Terms*—Chance-constrained programming, day-ahead scheduling, flexibility, model uncertainties, underground pumped hydro energy storage.**

NOMENCLATURE

A. Sets and Indices

T	Set of time steps, index t.
Ω	Set of stochastic scenario of exogenous variables, index ω.
H	Set of UPHES plants, index h.
N	Set of net head intervals, index n.
R	Set of reserve categories, index r.
$R^+ \subseteq R$	Set of upward reserve categories.
$R^- \subseteq R$	Set of downward reserve categories.

B. Decision Variables

res_r	Total reserve capacity allocated in reserve category r, (MW).
$res^{\mathrm{P}}_{h,r}, res^{\mathrm{T}}_{h,r}$	Reserve capacity allocated in pump (P) and turbine (T) mode by plant h in reserve category r, (MW).
$v^{\mathrm{res}}_{h,t,r}$	Additional displaced volume of water due to activation of reserves of plant h in reserve category r at time step t, (m³).
e^{DA}_t	Energy exchanged in the day-ahead market at time step t, (MWh).
$z^{\mathrm{P}}_{h,t}, z^{\mathrm{T}}_{h,t}$	Binary variables indicating the pump (P) and turbine (T) status of plant h at time step t.
$p^{\mathrm{P}}_{h,t}, p^{\mathrm{T}}_{h,t}$	Output power in pump (P) and turbine (T) modes of plant h at time step t, (MW).
$q^{\mathrm{P}}_{h,t}, q^{\mathrm{T}}_{h,t}$	Water flow rates in pump (P) and turbine (T) mode of plant h at time step t, (m³/s).
$v^{\mathrm{up}}_{h,t}, v^{\mathrm{low}}_{h,t}$	Water volume in the upper (up) and lower (low) basins of plant h at time step t, (m³).
$h^{\mathrm{up}}_{h,t}, h^{\mathrm{low}}_{h,t}$	Water head in the upper (up) and lower (low) basins of plant h at time step t, (m).
$h^{\mathrm{net}}_{h,t}$	Net head in plant h at time step t, (m).
$h^{\mathrm{loss}}_{h,t}$	Head loss in plant h at time step t, (m).
$d^{\mathrm{PHES}}_{h,t,n}$	Binary variable, equal to 1 if the net head of plant h is in interval n at time step t, and 0 otherwise.

C. Parameters

Δt	Temporal resolution of the optimization procedure, (h).
π_ω	Probability of scenario ω.
λ^{res}_r	Price for availability of reserve capacity in reserve category r, (€ /MW).
$\lambda^{\mathrm{DA}}_{\omega,t}$	Electricity price in the day-ahead energy-only market at time step t in scenario ω, (€ /MWh).
C^{op}_h	Operating costs of plant h, (€ /MWh).
$\Delta P^{P}_{h,r}, \Delta P^{\mathrm{T}}_{h,r}$	Ramping ability in pump (P) and turbine (T) mode of plant h in reserve category r, (MW).

Manuscript received October 31, 2018; revised April 2, 2019 and June 7, 2019; accepted July 12, 2019. Date of publication July 22, 2019; date of current version June 19, 2020. This article was supported by the Public Service of Wallonia (Belgium), within the framework of the Smartwater project. Paper no. TSTE-01086-2018. *(Corresponding author: Jean-François Toubeau.)*

J.-F. Toubeau, Z. De Grève, and F. Vallée are with the Electrical Power Engineering Unit, University of Mons, B-7000 Mons, Belgium (e-mail: jean-francois.toubeau@umons.ac.be; zacharie.degreve@umons.ac.be; francois.vallee@umons.ac.be).

P. Goderniaux is with the Geology and Applied Geology Unit, University of Mons, B-7000 Mons, Belgium (e-mail: pascal.goderniaux@umons.ac.be).

K. Bruninx is with the University of Leuven (KU Leuven) Energy Institute, TME Branch (Energy Conversion), B-3001 Leuven, Belgium, with Flemish Institute for Technological Research, B-2400 Mol, Belgium, and also with EnergyVille, B-3600 Genk, Belgium (e-mail: kenneth.bruninx@kuleuven.be).

Color versions of one or more of the figures in this article are available online at http://ieeexplore.ieee.org.

Digital Object Identifier 10.1109/TSTE.2019.2929687

$\overline{Q}_h^{\mathrm{P}}$, $\overline{Q}_h^{\mathrm{T}}$ Maximum water flow rates in pump (P) and turbine (T) mode of plant h, (m³/s).

$\overline{V}_h^{\mathrm{up}}$, $\overline{V}_h^{\mathrm{low}}$ Maximum water volume in the upper (up) and lower (low) basin of plant h, (m³).

V_h^{target} Target amount of water in the upper basin at the end of the optimization horizon of plant h, (m³).

$\underline{F}_{h,n}^{\mathrm{T}}, \overline{F}_{h,n}^{\mathrm{T}}$ Stepwise approximation of upper and lower bounds of the safe operating zone in turbine (T) mode for net head interval n, (MW).

$\underline{f}_{h,n}^{\mathrm{T}}, \overline{f}_{h,n}^{\mathrm{T}}$ Piecewise linear approximation of upper and lower bounds of safe operating zone in turbine (T) mode for net head interval n, (MW)

$\overline{A}_{h,n}^{\mathrm{T}}, \overline{B}_{h,n}^{\mathrm{T}}$ Slope and constant term of upper bound of safe operating zone in turbine (T) mode for net head interval n, (MW/m), (MW).

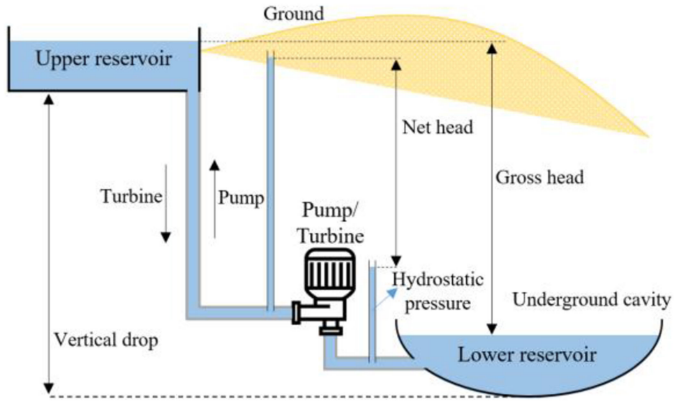

Fig. 1. Typical underground pumped hydro energy storage (UPHES) system.

I. Introduction

THE massive integration of electricity generation from renewable energy sources, such as solar and wind energy, poses significant challenges for power system operators. These resources are intrinsically uncertain and intermittent, which results in an increased need of flexibility to mitigate mismatches between electricity generation and consumption [1]. Pumped-hydro energy storage (PHES), a robust and mature technology currently representing over 99% of the worldwide installed storage capacity, may play a pivotal role in providing this flexibility [2]–[4]. Recent progresses in power electronics have indeed enabled PHES units to operate dynamically at variable speeds in both pump and turbine modes, thereby enhancing their operating range [5].

However, the potential of conventional PHES installations is constrained, since it requires a minimum height difference between both reservoirs. Conversely, in underground pumped storage hydropower (UPHES), as represented in Fig. 1, the upper reservoir is located at the surface or at shallow depth, while the lower one is underground, making this a viable alternative in flat regions [6]. Although this underground basin can be excavated, abandoned quarries and mines may be used, allowing significant investment cost reductions and, in some cases, to exploit the existing access to the grid [7], [8]. To the best of author's knowledge, there are currently no UPHES in operation, but different authors investigated the possibility to implement such systems in open pit or underground quarries, focusing on, e.g., geo-mechanical [9], [10] and hydrogeological issues [7], [11]. These studies highlight significant storage potential, even in relatively flat regions. For example, the capacity in Belgium's Walloon Region is assessed at 815 MW and 5000 MWh, distributed over 76 sites [12]. In the case study (Section IV), we describe a hypothetical UPHES unit, based on the characteristics of a potential site in Belgium.

In this paper, we study the multi-period, stochastic day-ahead scheduling problem faced by UPHES unit owners that jointly participate in energy and reserve markets. The profitability of UPHES plants strongly depends on the efficiency of the planning process governing its participation in energy and ancillary service markets. These schedules must indeed be determined optimally to fully exploit the limited hydro energy resource while satisfying hydraulic and electromechanical constraints, over an horizon of typically one day or one week. This gives rise to challenging optimization problems [13]–[15], which are discontinuous (due to the forbidden operating zones of the hydraulic machines to avoid cavitation, see Section II), nonlinear (to accurately represent, e.g., head dependencies), and non-convex (due to integer decision variables to discriminate the pumping, generating and idle operation modes), which must be solved under uncertainty (e.g., on market conditions).

To address these complex decision problems, researchers have deployed a wide range of techniques for both hydro generation and pumped storage plants. For example, dynamic programming has been used but its practical application is strongly affected by the curse of dimensionality [16], [17]. A nonlinear programming model is proposed in [18], but solving such nonlinear problems directly comes typically entails a high computational cost and the global optimality of the solution cannot be guaranteed [19]. Similarly, convergence issues in Lagrangian relaxation-based implementations [20], [21] motivated researchers to pursue other techniques. Meta-heuristics [22]–[24] were also tested, but such techniques do not provide any information about the solution optimality, which is moreover strongly dependent on the starting solution provided to the algorithm. Therefore, piecewise linear approximation-based formulations have been proposed using mixed-integer linear programming (MILP). These models have been progressively improved (with more tight and compact formulations) to solve the PHES scheduling problem with head-dependent characteristics more efficiently [25]–[35]. However, errors caused by the linearization, required to ensure computational tractability, of complex effects (i.e., nonlinear water levels within reservoirs, penstock head loss and head-dependent pump/turbine performance curves) may lead to infeasible solutions. In order to guarantee the feasibility of the PHES schedule, a MILP formulation considering conservative estimates of the output power range has been proposed in [36].

The common feature of all these models is that they assume that the characteristics of the hydro plants are perfectly known. However, for UPHES units, the geometry and hydraulic

properties of the underground cavity are typically unknown (Fig. 1). In such flooded cavities, water transfers rely on complex interactions between shafts, galleries, potentially collapsed chambers, and the adjacent porous and/or fractured rock structures. This leads to uncertainty on the UPHES state (such as the exact net head value), and thus on its safe operating range. Disregarding these model uncertainties may thus mislead the UPHES operator into believing that the obtained schedule satisfies all hydraulic and electromechanical constraints, while it may actually lead to infeasible (unsafe) solutions. Such a situation results in, e.g., an inability to meet day-ahead schedules and costly financial penalties in real-time or balancing markets.

The main contribution of this paper is the immunization of the UPHES day-ahead scheduling problem in energy and reserve capacity markets against infeasible operating conditions, arising from both the approximation of the UPHES nonlinear characteristics and the limited knowledge of the UPHES state (endogenous model uncertainties), by leveraging chance-constrained programming. Indeed, by defining a probability that constraint violations are kept smaller than a target value, the method allows managing the risk of obtaining infeasible operating schedules (that would lead to severe financial penalties), while avoiding to rely on conservative approaches, as in [36], which would prevent the UPHES to take full advantage of its flexibility, reducing its profitability.

An important advantage of the proposed procedure is that modeling errors and endogenous model uncertainties can be considered independently from the exogenous sources of uncertainty (that do not influence the UPHES state, such as market conditions), which are here modeled with scenarios to fully exploit the knowledge of the associated probability distributions (that can be efficiently forecasted [37], [38]). Results from a case study on a hypothetical UPHES plant on an actual candidate site demonstrate that the proposed chance-constrained method allows determining the risk attitude that maximizes profits, thereby outperforming their risk-neutral, deterministic equivalents.

The remainder of this paper is organized as follows. Section II introduces the rationale and principle of the proposed methodology, while Section III describes the mathematical formulation of the UPHES day-ahead scheduling problem, including the chance-constrained approach to deal with both modeling errors and endogenous system uncertainties. Section IV presents and discusses the computational results obtained for different risk-attitudes of the UPHES operator, and shows the robustness of the solution through an out-of-sample analysis. Finally, conclusions and potential outlooks for future research are given in Section V.

II. Motivation

When determining the operating schedule of any pumped storage system, which may be linked to a position in a day-ahead energy and/or ancillary service markets, the operator must take into account the technical constraints of the system. In addition to typical limits in terms of energy capacity and ramping abilities, the operation of hydraulic machines is governed by a three-dimensional relationship between the water flow, the output power and the net head. This function, referred to as the unit performance curve (UPC) describes the efficiency of the hydraulic machinery. Such a curve is illustrated in Fig. 2 for a typical reversible variable-speed Francis machine in turbine mode.

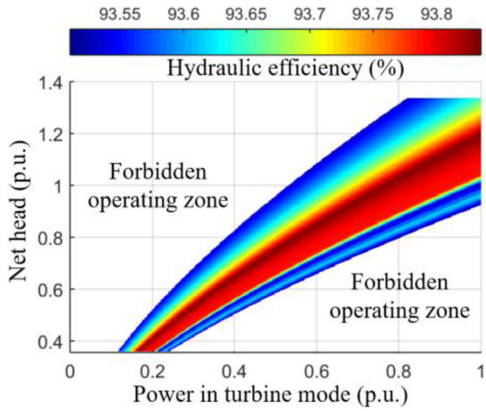

Fig. 2. Unit performance curve (UPC) of a Francis machine in turbine mode.

Aside from their complex water-power conversion characteristics, hydraulic machines are also characterized by two forbidden operating zones (Fig. 2). First, increasing the output power for a fixed net head value requires higher water flow rates, which ultimately leads to cavitation problems. Second, part-load operation (lower output power for a given net head value, i.e., lower water flow rates) gives rise to mechanical vibrations and severe erosion of the hydraulic system [39]. Note that the safe UPHES operating domain is not fixed, but depends on the net head value (since the latter defines the pressure conditions, and thus the stability margins of the hydraulic machine). An accurate description of the head-dependent UPCs is thereby essential to ensure that the resulting UPHES model leads to a reliable, feasible operating schedule and, thus, a profit-maximizing market participation. However, the inherent complexity to properly represent the nonlinear (non-concave and non-convex) UPCs requires relying on modeling approximations (Section III).

In real-life applications, the decision problem may be complicated by uncertainty on the real-time state of the system, e.g., due to the participation in operating reserve markets. Indeed, in this case the stochastic real-time activation of reserves impacts the net head available at each time step, which in turn determines the feasible operating region. In the specific case of UPHES, the possibly partially unknown internal physical characteristics (such as the exact geometry and the hydraulic behavior of underground cavities) may render the net head value itself uncertain, further complicating the scheduling problem faced by UPHES owners.

In this paper, we leverage chance-constrained programming to hedge the operating schedule of an UPHES against adverse effects associated with these uncertainties and the risk of infeasible operating schedules. The chance constraints introduced in Section III-D immunize the UPHES against infeasible schedules, arising from (i) the approximations of the unit performance curves (UPCs), (ii) the limited knowledge of the UPHES characteristics (endogenous uncertainties), and (iii) the uncertain future activation of operating reserves by limiting the operating region

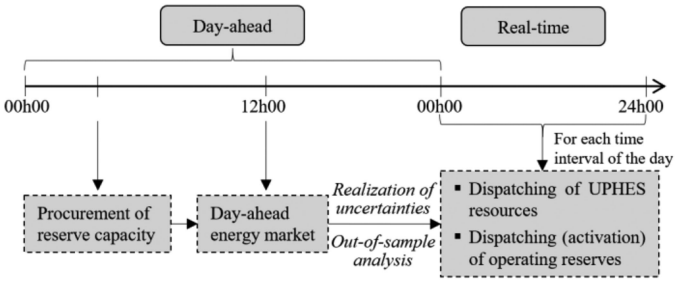

Fig. 3. Structure of the considered operating reserve and energy-only market and the associated day-ahead decision procedure of the UPHES owner.

of the UPHES. By reformulating the chance constraints as a set of convex constraints instead of relying on scenario-based techniques, we preserve computational resources to solve a NP-hard mixed integer problem. As such, this formulation provides an efficient framework to obtain the best trade-off between (i) the revenues in day-ahead energy and reserves markets and (ii) real-time penalties due to overly aggressive bidding strategies (for which the energy cannot be provided due to infeasible schedules), based on the risk-attitude of the UPHES owner.

III. Methodology

Below, we formulate the day-ahead scheduling problem faced by an operator of UPHES plants. The operator maximizes its profit in the day-ahead energy and reserve markets, considering modeling errors and endogenous model uncertainties (via chance-constraints), and exogenous sources of uncertainty, i.e., electricity prices in the day-ahead energy market (via representative scenarios). The UPHES owner is a price-taker in both reserve and energy markets.

The considered market structure is inspired by the European energy-only and reserve capacity markets, which are cleared sequentially via independent auctions [40]. In most countries, however, the reserve procurement currently takes place well before the day-ahead market clearing (e.g., week-ahead), which prevents storage resources to efficiently contribute due to the necessity to be continuously available during the whole contracting period [41]. To overcome this barrier, European regulatory bodies have recently defined guidelines [42] to clear the reserve capacity market on a daily basis, shortly before the energy market (Fig. 3).

Considering the limited delay between the clearing of both day-ahead markets and the strong link between operating reserves and arbitrage opportunities for an UPHES owner, we formulate the UPHES owner's participation in these markets as a single decision problem. In our formulation, the UPHES operator needs to be in balance in real-time, i.e., what is offered on all market floors must actually be supplied. However, due to approximation errors and uncertainties, it may happen that the UPHES is unable to meet its operating schedule, thereby facing imbalance penalties (relating to expensive adjustments in intraday or real-time balancing markets) that significantly exceed day-ahead energy prices. To mimic and quantify the impact of such real-time adjustments to the UPHES position, we perform out-of-sample simulations representing possible configurations of the (imperfectly known) underground reservoir, day-ahead electricity prices and real-time activation of reserves (Section IV).

A. Objective Function

The UPHES operator participates in both reserve and energy markets by deciding the charging (pump) and discharging (turbine) power in the form of quantity bids. We disregard uncertainty on the reserve capacity prices, assuming these may be predicted with high confidence. The day-ahead scheduling problem's objective therefore boils down to (1), where the UPHES operator maximizes its expected profit Φ^{A} based on (i) the revenues for the availability of up and down reserve capacity over the scheduling horizon, (ii) the revenues associated with energy sold and bought in the day-ahead electricity market, and (iii) the operating costs of the units:

$$\max \Phi^{\mathrm{A}} = \sum_{r\in R} \underbrace{24 \cdot \lambda_r^{\mathrm{res}} \cdot res_r}_{(i)} + \sum_{t\in T} \left[\sum_{\omega\in\Omega} \underbrace{\pi_\omega \cdot \lambda_{t,\omega}^{\mathrm{DA}} \cdot e_t^{\mathrm{DA}}}_{(ii)} - \sum_{h\in H} \underbrace{C_h^{op} \cdot \left(p_{h,t}^{\mathrm{T}} + p_{h,t}^{\mathrm{P}}\right)}_{(iii)} \right] \tag{1}$$

We assume that (i) the participation in the balancing market is budget-neutral (the expected profit for the activation of reserves is offset by the UPHES operating costs) and (ii) the operator must provide a feasible operating schedule, i.e., that it may not willingly incur imbalance penalties, hence, these penalties do not appear in the objective function (1).

B. Energy Balance and Reserve Allocation Constraints

Constraint (2) imposes that the energy exchanged on the electricity market is balanced by the available resources:

$$e_t^{\mathrm{DA}} = \Delta t \cdot \sum_{h\in H} \left(p_{h,t}^{\mathrm{T}} - p_{h,t}^{\mathrm{P}}\right) \qquad \forall t \tag{2}$$

The flexibility of the PHES units can be valued in the reserve market. The proposed formulation aims at determining the optimal reserve capacity in the different products $r \in R$, through a profit-maximizing allocation of the UPHES flexibility res_r over the scheduling horizon (3). Upward reserve capacity can be provided either by increasing the generated power in turbine mode or by reducing the pumping power. Similarly, downward reserves are supplied by lowering the turbine power or by increasing up the pump output power:

$$\sum_{h\in H} \left(res_{h,t,r}^{\mathrm{T}} + res_{h,t,r}^{\mathrm{P}}\right) = res_r \qquad \forall t, r \tag{3}$$

Moreover, the reserve capacity allocated to each unit is limited by its ramping ability and the operational requirements of the different reserve categories. Indeed, up and down services are classified into different categories according to their response speed [43]. Frequency containment reserves (FCR) are automatically activated to alleviate momentary frequency deviations. Then, automatic frequency restoration reserves (aFRR) are dispatched

to free up FCR capacity for new contingencies. If the problem persists, the system operator requests the activation of manual frequency restoration reserves (mFRR), which remain online until the situation is resolved. Upward FCR (*fu*) and downward FCR (*fd*) must be fully activated in 30 seconds, upward aFRR (*au*) and downward aFRR (*ad*) in 7.5 minutes, whereas upward mFRR (*mu*) and downward mFRR (*md*) in 15 minutes.

$$res^{i}_{h,t,r} \leq z^{i}_{h,t} \cdot \Delta R^{i}_{h,r} \quad \forall h,t,i \in \{\mathrm{T},\mathrm{P}\}, r \in \{fu,fd\} \quad (4)$$

$$res^{i}_{h,t,fu} + res^{i}_{h,t,au} \leq z^{i}_{h,t} \cdot \Delta R^{i}_{h,au} \quad \forall h,t,i \in \{\mathrm{T},\mathrm{P}\} \quad (5)$$

$$res^{i}_{h,t,fd} + res^{i}_{h,t,ad} \leq z^{i}_{h,t} \cdot \Delta R^{i}_{h,ad} \quad \forall h,t,i \in \{\mathrm{T},\mathrm{P}\} \quad (6)$$

$$\sum_{r \in R^{+}} res^{i}_{h,t,r} \leq z^{i}_{h,t} \cdot \Delta R^{i}_{h,mu} \quad \forall h,t,i \in \{\mathrm{T},\mathrm{P}\} \quad (7)$$

$$\sum_{r \in R^{-}} res^{i}_{h,t,r} \leq z^{i}_{h,t} \cdot \Delta R^{i}_{h,md} \quad \forall h,t,i \in \{\mathrm{T},\mathrm{P}\} \quad (8)$$

Constraint (4) ensures that the UPHES owner does not allocate more reserve capacity to the FCR category than it can provide within 30 seconds (according to the UPHES ramping abilities). Equations (5)–(6) allow offering the remaining ramping capacity available in a 7.5 minutes time frame as aFRR. Similarly, Constraints (7)–(8) ensure that the offered reserve capacity complies with the ramping requirements of the mFRR.

C. Technical Constraints of PHES Technology

The hydraulic machine is constrained by water discharges limitations in pump (9) and turbine (10) mode:

$$q^{\mathrm{P}}_{h,t} \leq z^{\mathrm{P}}_{h,t} \cdot \overline{Q}^{\mathrm{P}}_{h} \quad \forall h,t \quad (9)$$

$$q^{\mathrm{T}}_{h,t} \leq z^{\mathrm{T}}_{h,t} \cdot \overline{Q}^{\mathrm{T}}_{h} \quad \forall h,t \quad (10)$$

The water volumes in the upper (11) and lower (12) reservoirs allow coupling the charge and discharge decisions across the scheduling horizon:

$$v^{\mathrm{up}}_{h,t} = v^{\mathrm{up}}_{h,t-1} + \left(q^{\mathrm{P}}_{h,t} - q^{\mathrm{T}}_{h,t}\right) \cdot \Delta t \quad \forall h,t \quad (11)$$

$$v^{\mathrm{low}}_{h,t} = v^{\mathrm{low}}_{h,t-1} + \left(q^{\mathrm{T}}_{h,t} - q^{\mathrm{P}}_{h,t}\right) \cdot \Delta t \quad \forall h,t \quad (12)$$

When scheduling PHES plants that are providing upward reserves, one should ensure that sufficient water is stored in the upper reservoir and/or that the lower basin is able to accommodate the additional water inflow. Similarly, for the reliable provision of downward reserves, the formulation should guarantee that enough water is available in the lower basin and/or that the upper reservoir is sufficiently large to store the transferred water. These limits on the water volumes have to be respected at each time step, in the worst-case scenario, i.e., activation of all reserves in one direction [44]:

$$\underline{V}^{\mathrm{up}}_{h} + \sum_{t'=1}^{t} \sum_{r \in R^{+}} v^{\mathrm{res}}_{h,t',r} \leq v^{\mathrm{up}}_{h,t} \leq \overline{V}^{\mathrm{up}}_{h} - \sum_{t'=1}^{t} \sum_{r \in R^{-}} v^{\mathrm{res}}_{h,t',r} \quad \forall h,t \quad (13)$$

$$\underline{V}^{\mathrm{low}}_{h} + \sum_{t'=1}^{t} \sum_{r \in R^{+}} v^{\mathrm{res}}_{h,t',r} \leq v^{\mathrm{low}}_{h,t} \leq \overline{V}^{\mathrm{low}}_{h} - \sum_{t'=1}^{t} \sum_{r \in R^{+}} v^{\mathrm{res}}_{h,t',r} \quad \forall h,t \quad (14)$$

The additional water volumes $v^{\mathrm{res}}_{h,t',r}$ due to the activation of reserves are obtained as follows

$$v^{\mathrm{res}}_{h,t',r} = \frac{3600 \cdot 10^{6} \cdot \left(res^{\mathrm{T}}_{h,t',r} + res^{\mathrm{P}}_{h,t',r}\right)}{\eta_{h,t'} \cdot \rho \cdot g \cdot h^{\mathrm{net}}_{h,t'}} \quad (15)$$

where $g = 9.81$ m/s² and ρ is the fluid density (1000 kg/m³). To avoid nonlinearities in (15), the efficiency $\eta_{h,t'}$ and net head value $h^{\mathrm{net}}_{h,t'}$ are assumed to be constant. Practically, conservative values are considered to prevent infeasibilities (e.g., by overestimating water volumes when considering the maximum limits of the basins).

The water volume in the upper reservoir at the end of the scheduling horizon (i.e., the financial value of the energy stored in the UPHES beyond the scheduling horizon) is enforced via a target value:

$$v^{\mathrm{up}}_{h,t=T} \geq V^{\mathrm{target}}_{h} \quad \forall h \quad (16)$$

The height of the water column in the upper (17) and lower (18) reservoirs is a function of the water volume in the corresponding reservoir. The complexity of these functions is defined by the geometry of the natural cavities used as reservoirs, as well as the water interactions with the surrounding environment. Due to friction and turbulence within the penstock, the net head is always lower than the gross head (20). This penstock head loss (19) is usually modeled as a quadratic function of the water flow [17]:

$$h^{\mathrm{up}}_{h,t} = f^{\mathrm{up}}_{h}\left(v^{\mathrm{up}}_{h,t}\right) \quad \forall h,t \quad (17)$$

$$h^{\mathrm{low}}_{h,t} = f^{\mathrm{low}}_{h}\left(v^{\mathrm{low}}_{h,t}\right) \quad \forall h,t \quad (18)$$

$$h^{\mathrm{loss}}_{h,t} = c^{\mathrm{loss}}_{h} \cdot \left(q^{\mathrm{T}}_{h,t} + q^{\mathrm{P}}_{h,t}\right)^{2} \quad \forall h,t \quad (19)$$

$$h^{\mathrm{net}}_{h,t} = \underbrace{h^{\mathrm{up}}_{h,t} - h^{\mathrm{low}}_{h,t}}_{\text{gross head}} - h^{\mathrm{loss}}_{h,t} \quad \forall h,t \quad (20)$$

The three one-dimensional nonlinear functions (17), (18), and (19) are, in this work, all approximated via piecewise linear interpolation, as proposed in [36].

As represented in Fig. 2, hydraulic pump-turbine machines are characterized by three-dimensional nonlinear relations, referred to as unit performance curves (UPCs), linking the net head, the output power, and the unit outflow in pump (21) and turbine (22) mode. These UPCs thus define the hydraulic efficiency of the PHES plant:

$$p^{\mathrm{P}}_{h,t} = f^{\mathrm{UPC},P}_{h}\left(q^{\mathrm{P}}_{h,t}, h^{\mathrm{net}}_{h,t}\right) \quad \forall h,t \quad (21)$$

$$p^{\mathrm{T}}_{h,t} = f^{\mathrm{UPC},T}_{h}\left(q^{\mathrm{T}}_{h,t}, h^{\mathrm{net}}_{h,t}\right) \quad \forall h,t \quad (22)$$

In order to avoid a nonlinear formulation, the UPCs (21) and (22) are linearly approximated. Considering the computational

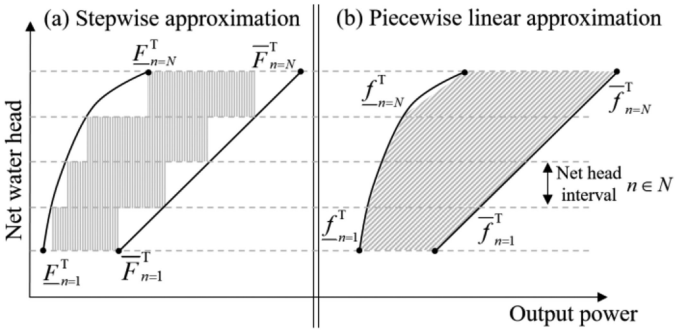

Fig. 4. Approximation methods of the turbine performance curve.

burden, we follow the idea in [29], [36], [1] by discretizing the net head into several subintervals $n \in N$. We use one-dimensional linear functions in each net water head subinterval n to approximate the relationship between the output power and the water discharge.

Furthermore, as indicated by the white areas in Fig. 2, PHES units are also characterized by forbidden zones, defined by stability limits of the hydraulic machine. These restricted zones lead to a discontinuous optimization problem that requires two binary variables $z^{\mathrm{P}}_{h,t}$ and $z^{\mathrm{T}}_{h,t}$ to discriminate operation modes (pump, turbine and idle) at each time step.

$$z^{\mathrm{T}}_{h,t} + z^{\mathrm{P}}_{h,t} \leq 1 \qquad \forall h,t \tag{23}$$

In addition, the resulting safe operating ranges of UPHES plants (24)–(25) must account for the capacity allocated to provide operating reserves. Specifically, UPHES capacity may not be simultaneously reserved for both reserve provision and arbitrage purposes, such that the feasibility of activating scheduled UPHES reserve capacity is always guaranteed:

$$z^{\mathrm{P}}_{h,t} \cdot \underline{p}^{\mathrm{P}}_{h,t} + \sum_{r\in R^+} res^{\mathrm{P}}_{h,r} \leq p^{\mathrm{P}}_{h,t} \leq z^{\mathrm{P}}_{h,t} \cdot \overline{p}^{\mathrm{P}}_{h,t} - \sum_{r\in R^-} res^{\mathrm{P}}_{h,r} \qquad \forall h,t \tag{24}$$

$$z^{\mathrm{T}}_{h,t} \cdot \underline{p}^{\mathrm{T}}_{h,t} + \sum_{r\in R^-} res^{\mathrm{T}}_{h,r} \leq p^{\mathrm{T}}_{h,t} \leq z^{\mathrm{T}}_{h,t} \cdot \overline{p}^{\mathrm{T}}_{h,t} - \sum_{r\in R^+} res^{\mathrm{T}}_{h,r} \qquad \forall h,t \tag{25}$$

The limits on the UPHES safe operating zones, i.e., $[p^{\mathrm{T}}_{h,t},\ \bar{p}^{\mathrm{T}}_{h,t}]$ in turbine and $[p^{\mathrm{P}}_{h,t},\ \bar{p}^{\mathrm{P}}_{h,t}]$ in pump operation, vary nonlinearly with the net head, and must therefore be considered as state variables. In what follows, we discuss two options to model these zones in turbine mode (25), which differ by their (i) accuracy and complexity and (ii) computational burden. Obtaining the equivalent constraints for the pump mode (24) is straightforward.

1) Stepwise Approximation of Operating Zones: In this first method depicted in Fig. 4(a), the safe operating limitations $\underline{p}^{\mathrm{T}}_{h,t}$ and $\bar{p}^{\mathrm{T}}_{h,t}$ defined in (25), are respectively approximated by constant values $\underline{F}^{\mathrm{T}}_{h,n}$ and $\bar{F}^{\mathrm{T}}_{h,n}$ within each net head interval $n \in N$:

$$p^{\mathrm{T}}_{h,t} - \sum_{r\in R^-} res^{\mathrm{T}}_{h,r} \geq \underline{F}^{\mathrm{T}}_{h,n} - \left(1 - z^{\mathrm{T}}_{h,t}\right)\cdot M - \left(1 - d^{\mathrm{PHES}}_{h,t,n}\right)\cdot M \quad \forall h,t,n \tag{26}$$

$$p^{\mathrm{T}}_{h,t} + \sum_{r\in R^+} res^{\mathrm{T}}_{h,r} \leq \overline{F}^{\mathrm{T}}_{h,n} + \left(1 - d^{\mathrm{PHES}}_{h,t,n}\right)\cdot M \quad \forall h,t,n \tag{27}$$

To ensure that the adequate power bounds are considered (based on the net head value), these constraints will only be binding when the binary state variable $d^{\mathrm{PHES}}_{h,t,n}$ is equal to 1, and will otherwise be deactivated by the inclusion of the M penalty ($M > \bar{F}^{\mathrm{T}}_{h,n=N}$). In addition, the minimum bound is only imposed when the unit is actually generating ($z^{\mathrm{T}}_{h,t} = 1$), thereby ensuring, along with (10) and (22), that the turbine power is equal to 0 when the unit is pumping or offline.

2) Piecewise Linear Approximation of Operating Zones: In the stepwise formulation, the safe operating zone within each net head interval $n \in N$ is approximated by a rectangle, which may be conservative. Henceforth, this method is improved by approximating the operating zone by a more general (but more complex) polygon [31]. As represented in Fig. 4(b), the operating limits are thus represented as linear and monotonic functions $\underline{f}^{\mathrm{T}}_{h,n}$ and $\bar{f}^{\mathrm{T}}_{h,n}$, which allows representing the UPCs more accurately:

$$p^{\mathrm{T}}_{h,t} - \sum_{r\in R^-} res^{\mathrm{T}}_{h,r} \geq \underbrace{\underline{A}^{\mathrm{T}}_{h,n}.h^{\mathrm{net}}_{h,t} + \underline{B}^{\mathrm{T}}_{h,n}}_{\underline{f}^{\mathrm{T}}_{h,n}} - \left(1 - z^{\mathrm{T}}_{h,t}\right)\cdot M - \left(1 - d^{\mathrm{PHES}}_{h,t,n}\right)\cdot M \quad \forall h,t,n \tag{28}$$

$$p^{\mathrm{T}}_{h,t} + \sum_{r\in R^+} res^{\mathrm{T}}_{h,r} \leq \underbrace{\overline{A}^{\mathrm{T}}_{h,n}.h^{\mathrm{net}}_{h,t} + \overline{B}^{\mathrm{T}}_{h,n}}_{\bar{f}^{\mathrm{T}}_{h,n}} + \left(1 - d^{\mathrm{PHES}}_{h,t,n}\right)\cdot M \quad \forall h,t,n \tag{29}$$

Note that both approximation methods used to represent the nonlinear UPC functions are inherently linked to a discretization error (whose magnitude depends on the number of net head intervals N). This error is quantified in the case study (Section IV-A), where it is referred to as approximation error of 'type 1'.

D. Accounting for Endogenous Model Uncertainties

The UPHES model is characterized by structural uncertainty associated with the geometry and hydraulic properties of the underground basin, as well as approximation errors from linearizing the non-linear UPCs. Both effects boil down to an uncertain value of the net head $h^{\mathrm{net}}_{h,t}$, which is translated into uncertainty regarding the safe operating zones (feasible region) and the associated efficiency of the hydraulic machine. To hedge against infeasibilities, the restricted operating zone constraints (24)–(25) are therefore revised in [36] by using a conservative

[1]Note that other approximations, such as meshing and triangulation techniques [34]–[35], exist.

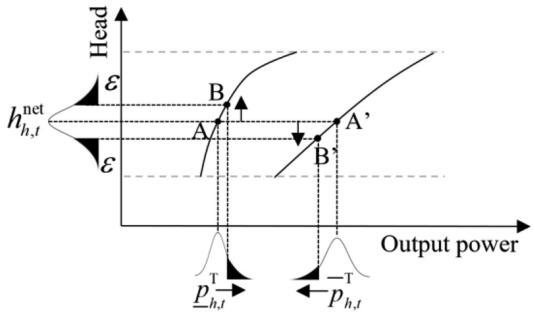

Fig. 5. Illustration of the chance-constrained programming approach, which infers tighter bounds on the safe output power range.

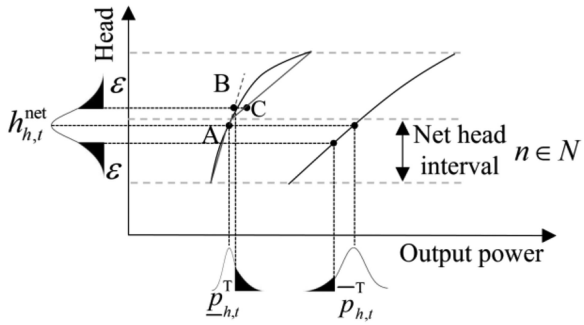

Fig. 6. Discretization errors in the piecewise linear formulation.

upper bound of the unit output power, thereby guaranteeing the feasibility of the resulting PHES with respect to the non-linear UPCs. However, in addition to its conservativeness, such an approach does not allow properly considering endogenous model uncertainties.

In this paper, chance-constrained programming is therefore leveraged to hedge against both formulation approximations and model uncertainties. As depicted in Fig. 5 for the turbine operation mode, the principle is to convert the uncertain net head distribution into uncertain power limitations, by using the UPCs. Based on the risk-attitude ε of the UPHES operator, the latter distributions are then exploited to infer tighter (safer) operating bounds on the operational range of the unit. In this way, in the risk-neutral case, based on the net head value $h^{\text{net}}_{h,t}$, the minimum and maximum power limits are respectively given by points A and A'. If the UPHES operator is risk-averse, the bounds are tightened and given by points B and B'. Overall, the chance constraints thereby ensure that the restricted operating zone constraints are satisfied with a predefined probability 1-ε over the uncertainty space (i.e., the net-head distribution's domain). Note that if $\varepsilon = 0.5$, a chance constraint is identical to its deterministic equivalent.

In this paper, chance constraints are reformulated analytically. Considering the simplified stepwise approximation (26)–(27) and the more complex piecewise linear model (28)–(29), we obtain two different reformulations of the problem. As demonstrated below, the stepwise formulation allows the chance constraints to be analytically recast as linear constraints, whereas the piecewise linear approach yields a second-order cone program [44]. Both problems can be solved efficiently using off-the-shelf solvers, as illustrated in our case study (Section IV). The chance constraints and their analytical reformulation are presented for the upper limit in turbine mode, but the equations can be straightforwardly adapted for the lower limit in turbine mode and the pump operation.

1) Stepwise Approximation of Operating Zones: Constraint (27) is reformulated as a chance constraint:

$$\Pr\left(p^{\mathrm{T}}_{h,t} + \sum_{r\in R^+} res^{\mathrm{T}}_{h,r} \le \left(1+\bar{\delta}^{\mathrm{T}}\right)\cdot \overline{F}^{\mathrm{T}}_{h,n} + \left(1-d^{\mathrm{PHES}}_{h,t,n}\right)\cdot M\right) \ge 1-\varepsilon \quad \forall h,t,n \tag{30}$$

The uncertainty associated with the power limits is assumed to follow a normal distribution, i.e., $\bar{\delta}^{\mathrm{T}} \sim N\,(0, (\bar{\sigma}^{\mathrm{T}})^2)$. Henceforth, for $1-\varepsilon \ge 0.5$, the chance constraints (30) can be analytically reformulated as a linear constraint [45]:

$$p^{\mathrm{T}}_{h,t} + \sum_{r\in R^+} res^{\mathrm{T}}_{h,r} \le \overline{F}^{\mathrm{T}}_{h,n} + \left(1-d^{\mathrm{PHES}}_{h,t,n}\right)\cdot M - \Phi^{-1}(1-\varepsilon)\cdot\bar{\sigma}^{\mathrm{T}} \quad \forall h,t,n \tag{31}$$

where $\Phi^{-1}(1-\varepsilon)$ is the $(1-\varepsilon)$-quantile of the standard normal distribution.

2) Piecewise Linear Approximation of Operating Zones: Constraint (29) is reformulated as follows:

$$\Pr\left(p^{\mathrm{T}}_{h,t} + \sum_{r\in R^+} res^{\mathrm{T}}_{h,r} \le \left(1+\bar{\delta}^{\mathrm{T}}\right)\cdot \overline{A}^{\mathrm{T}}_{h,n}\cdot h^{\mathrm{net}}_{h,t} + \overline{B}^{\mathrm{T}}_{h,n} + \left(1-d^{\mathrm{PHES}}_{h,t,n}\right)\cdot M\right) \ge 1-\varepsilon \quad \forall h,t,n \tag{32}$$

Contrary to the previous formulation (30) where the uncertain variable was additive, the uncertainty $\bar{\delta}^{\mathrm{T}}$ is here proportional to the net head. These chance constraints (32) can no longer be recast as simple linear constraints, but can be rewritten as second-order conic (SOC) constraints [45]:

$$p^{\mathrm{T}}_{h,t} + \sum_{r\in R^+} res^{\mathrm{T}}_{h,r} \le \overline{A}^{\mathrm{T}}_{h,n}\cdot h^{\mathrm{net}}_{h,t} + \overline{B}^{\mathrm{T}}_{h,n} + \left(1-d^{\mathrm{PHES}}_{h,t,n}\right)\cdot M - \Phi^{-1}(1-\varepsilon)\cdot\xi_{h,t,n} \quad \forall h,t,n \tag{33}$$

$$\xi^2_{h,t,n} \ge \left(\bar{\sigma}^{\mathrm{T}}\cdot \overline{A}^{\mathrm{T}}_{h,n}\cdot h^{\mathrm{net}}_{h,t}\right)^2 \quad \forall h,t,n \tag{34}$$

where $\xi_{h,t,n}$ is an auxiliary decision variable. The resulting formulation is a mixed integer quadratically-constrained problem (MIQCP) that can be solved with commercial off-the-shelf solvers such as CPLEX.

Note that both chance-constrained formulations yield discretization errors when the distribution characterizing the net head uncertainty covers multiple intervals $n \in N$ (Fig. 6). Indeed, in the piecewise linear model, the lower bound of the output power (curve on the left, Fig. 6) should be given by point C. However, in the proposed formulation, the bound is actually given by point B (pertaining to the associated adjacent segment), which decreases the conservativeness of the chance-constrained model. Since the risk-attitude ε (and thus the degree of

conservativeness of the procedure) can be freely selected, the impact of this discretization error on the UPHES operating schedules can be controlled by the operator. We will return to this issue in our case study (Section IV-A), where it is referred to as approximation error of 'type 2'.

IV. Case Study

The proposed model is applied to a hypothetical UPHES system, using an existing underground quarry as lower reservoir, to evaluate its practicality. In order to focus on the chance constraints and both approximations of the UPCs, a single UPHES plant is studied on a specific day. The vertical drop between both reservoirs is 90 m, where the lower one is a former underground mine. The complex underground environment is known with low certainty (approximate volume of 920,000 m³). The surface of the rectangular-shaped upper reservoir, i.e., 30,625 m² (for a volume of 225,000 m³), is relatively limited, which induces significant head variations (see Section IV-A). The standard deviation of the distribution characterizing the net head uncertainty is equal to $\sigma_{\text{opt}} = 0.025$, which corresponds to a variation of 2.25 m for a net head of 90 m. The UPHES nameplate capacity is equal to 10 MW in both pump and turbine modes. The operating costs are equal to 4 € /MWh in both pump and turbine modes.

Electricity prices in the day-ahead energy market are based on BELPEX data, and fluctuate between 39.9 € /MWh (5 a.m.) and 80.3 € /MWh (8 p.m.). Regarding operating reserves, FCR is valued at 10 € /MW/h, aFRR at 12.5 € /MW/h, and mFRR at 5 € /MW/h.

We study the performance of the UPHES scheduling problem based on the stepwise approximation and piecewise linear model for different risk-attitudes ε. Recall that if $\varepsilon = 0.5$, the formulation is identical to the deterministic problem without chance constraints. Both formulations are mixed-integer, and the gap tolerance of the solver is fixed at 0.5%. The models are implemented using Julia/JuMP, and solved using CPLEX 12.8 on an Intel Core$^{\text{TM}}$ i7-3770 CPU @ 3.4 GHz with 16 Gb of RAM.

In what follows, we first quantify the modeling errors associated with both stepwise and piecewise linear models for different input parameters, and we derive the best configuration to have a compromise between modeling accuracy and computational burden (Section IV-A). Then, a Monte Carlo out-of-sample analysis (in which uncertainties are represented using many representative scenarios) is performed to evaluate the feasibility and cost-efficiency of the solutions obtained for different risk-attitudes of the UPHES operator (Section IV-B). This analysis allows quantifying real-time imbalances (which are not included in the objective function), so as to determine the trade-off between the risk of infeasible operating schedules and the profits in the day-ahead (energy and reserve) markets. Finally, this out-of-sample analysis is extended to evaluate the robustness of the Gaussian assumption for representing model uncertainties. To that end, the optimal scheduling is tested against non-Gaussian realizations of uncertain parameters (Section IV-C).

A. Impact of Modeling Errors

Due to the limited surface of the reservoirs, the net head varies between 87 and 97 m (a fluctuation of more than 10% of the nominal value). This induces important variations of the safe operating zones, which necessitates to accurately represent the UPCs. A sensitivity analysis is thus performed to quantify the effect of the number of net head intervals N on (i) the simulation time, (ii) the approximation error of 'type 1' $e_{\text{approx.1}}$, i.e., the difference between the actual UPC and the stepwise or piecewise linear approximation presented in Fig. 4, and (iii) the approximation error of 'type 2' $e_{\text{approx.2}}$, i.e., the difference between points B and C in Fig. 6. It is important to mention that $e_{\text{approx.1}}$ depends only on N, whereas $e_{\text{approx.2}}$ depends on both N and the risk level ε. Mathematically, these approximation errors may be defined as in Eq. (35) and (36), where they are averaged over the scheduling horizon (aggregating contributions of both operating modes). The results are provided in Table I.

TABLE I
Modeling Errors for Different Number of Head Intervals N and Risk-Attitudes ε

		Stepwise approximation			Piecewise linear approximation		
N	ε	Time [s]	$e_{\text{approx.1}}$ [MW]	$e_{\text{approx.2}}$ [MW]	Time [s]	$e_{\text{approx.1}}$ [MW]	$e_{\text{approx.2}}$ [MW]
1	0.1	0.2	1.54	n/a	2.6	0.07	n/a
	0.01	0.2			2.8		
2	0.1	16.5	0.81	0.10	35.5	0.04	0.12
	0.01	5.5		0.20	37.9		0.25
3	0.1	119.9	0.54	0.19	206.1	0.04	0.01
	0.01	38.0		0.19	183.7		0.05
4	0.1	340.5	0.39	0.11	609.4	0.04	0.01
	0.01	141.0		0.12	406.6		0.03
5	0.1	1045.1	0.33	0.16	5146.7	0.04	0.01
	0.01	786.9		0.17	2740.2		0.02

$$e_{\text{approx.1}} = \sum_{t \in T} \frac{1}{T} \left(\left| \underline{p}^{\text{T}}_{\text{model},t} - \underline{p}^{\text{T}}_{\text{actual},t} \right| + \left| \overline{p}^{\text{P}}_{\text{model},t} - \overline{p}^{\text{P}}_{\text{actual},t} \right| \right) \tag{35}$$

$$e_{\text{approx.2}} = \sum_{t \in T} \frac{1}{T} \left(\left| \underline{p}^{\text{T}}_{B,t} - \underline{p}^{\text{T}}_{C,t} \right| + \left| \overline{p}^{\text{P}}_{B,t} - \overline{p}^{\text{P}}_{C,t} \right| \right) \tag{36}$$

The piecewise linear approximation allows accurately representing the UPCs, whereas the stepwise model is a conservative alternative that reduces the feasible operating region. In that regard, for the piecewise linear model, even a single net head interval leads to a limited approximation error of 'type 1', i.e., 0.07 MW in average for a 10 MW UPHES plant. This error then decreases with the number of net head intervals N. Note furthermore that this type of approximation error does not lead to infeasible operating schedules, assuming one knows the true UPC and the system state. Indeed, these approximation errors only reduce the UPHES operating range, hence may lead to foregone profits, but do not put the UPHES owner at risk of scheduling its unit outside of the safe operating range.

The approximation error of 'type 2' arises when $N > 1$ (when the true safe operating limit is given by the adjacent segment). In this specific case, the piecewise model (accounting for both approximation errors) with $N = 2$ is actually worse than the piecewise approximation with a single segment, especially if the UPHES owner is risk-averse. As illustrated in Fig. 6, the difference between points B and C increases with the risk-aversion ($\varepsilon \to 0$). However, this error is in general lower than the modeling

TABLE II
COMPARISON OF THE RELIABILITY AND PROFIT OF THE UPHES OPERATOR FOR THE TWO APPROXIMATION APPROACHES AND DIFFERENT RISK-ATTITUDES OF THE UPHES OWNER

	Risk ε	Day-ahead optimization		Out-of-sample results							
		Expected Profit [€]	Computation Time [s]	Reliability [%]	Minimum Profit [€]	Average Profit [€]	Maximum Profit [€]	Res [€]	DAM [€]	OpCosts [€]	Average RT penalties [€]
Stepwise approximation	0.5	2141.2	96	83.2	152.2	1860.0	2141.2	648.0	2095.7	-602.5	-281.2
	0.3	2075.0	62	85.3	293.9	1844.0	2075.0	552.7	2129.4	-607.1	-231.0
	0.1	1953.9	107	95.8	1183.1	1919.2	1953.9	415.0	2131.8	-593.0	-34.6
	0.01	1891.5	32	97.6	852.4	1861.2	1891.5	0	2285.4	-393.9	-30.3
	0.001	1877.5	14	98.7	1192.6	1868.8	1877.5	0	2264.3	-386.9	-8.7
Piecewise linear approximation	0.5	2375.5	534	68.1	-365.7	1736.5	2350.6	999.8	1959.8	-584.0	-639.1
	0.3	2301.8	256	75.1	-181.6	1881.9	2301.8	865.3	2028.4	-591.4	-419.9
	0.1	2162.1	208	85.9	41.8	1944.3	2162.1	653.4	2112.6	-603.8	-217.9
	0.01	1894.5	163	97.7	912.4	1872.3	1894.5	0	2294.0	-399.5	-22.1
	0.001	1872.5	74	99.8	1338.5	1870.4	1872.5	0	2259.6	-387.2	-2.1

approximations of UPCs, and is compensated by the fact that risk-averse policies reduce the operating range. Note, however, that if these discretization errors of 'type 2' would be significant, an operator may obtain infeasible dispatch schedules.

Overall, the risk-attitude ε therefore needs to be adjusted (Section IV-B) to find the trade-off between conservativeness and economic performance. The results also show that $N = 3$ offers good characteristics in terms of computation burden and modeling accuracy, hence, this number of head intervals will be used in the subsequent simulations.

B. Balancing the Risk of Infeasible Operating Schedules and Operating Profit

In Table II, we summarize the results of the 10 numerical simulations (performed for the 2 different formulations and 5 risk attitudes ε) of the UPHES operator. Results include (i) the computation time and the profit that is expected in the day-ahead scheduling procedure, (ii) the operating profits and costs as obtained from an out-of-sample analysis (see below) and (iii) the reliability of each result (i.e., the percentage of samples for which all the operating constraints are satisfied). The profit is split between the revenues associated with the provision of regulation reserve capacity (Res), arbitrage in the day-ahead market (DAM), operational costs (opCosts) and the financial penalties in the balancing market that vary among scenarios (RT penalties). These penalties result in variability in the profit that can be actually generated, which is here described with its minimum, average and maximum values.

The performance of the day-ahead scheduling is tested against possible realizations (scenarios) of the uncertainties through a Monte Carlo out-of-sample analysis. Each sample represents a possible configuration of the underground reservoir (which will infer different net head dependencies), along with a scenario of day-ahead electricity prices and of the real-time activation of reserves $r \in R$. The number of samples N_s in the out-of-sample analysis is fixed to 100,000 in order to guarantee that the ex-post reliability (i.e., percentage of scenarios in which the UPHES owner does not pay any imbalance penalties) is accurately estimated. Moreover, this ensures that the width of the 95% confidence interval around the ex-post average profit never exceeds 3€ (i.e., a deviation of at most 0.15%) for the 10 cases simulated in Table II. Practically, this confidence interval Δ is given by [46]:

$$\Delta = \frac{z_{1-\alpha/2} \cdot \sigma_{out}}{\sqrt{N_s}} \tag{37}$$

where σ_{out} is an estimator of the standard deviation (computed on the N_s out-of-sample values of the profit), and $z_{1-\alpha/2}$ is the inverse of the standard normal cumulative probability density function evaluated at $1 - \alpha/2$ (where α is here set to 0.05).

For each sample, the power output (scheduled at the end of the optimization) is adjusted based on the real-time contribution of reserves. Similarly, the UPHES system state and forbidden zones are also recomputed using the actual UPCs, which allows determining the actual water volumes within reservoirs and identifying whether the actual output power is in the allowed range. If not (because approximation errors and model uncertainties were not properly considered in the optimization), the operator must deviate in real-time from its balanced position to avoid damage to the hydraulic equipment and face the resulting financial penalties in the real-time market. These imbalance penalties are set to 200 € /MWh. In what follows, we discuss several trends that can be identified in the results summarized in Table II.

First, the design parameters selected in Section IV-A allow keeping the computation time below 10 minutes for both UPCs approximations, which permits the practical utilization of the tool for solving the day-ahead UPHES scheduling problem. Interestingly, the time tends to decrease for risk-averse strategies (whereas the problem size is independent of the risk levels ε), suggesting that trade-off between profits in reserves and energy markets is then easier to find (more constrained optimization problem).

Second, the piecewise linear approximation allows exploiting the flexibility of the UPHES more aggressively due to the more accurate description of the UPCs. Fig. 7 illustrates the impact of different ε-values on the feasible pump operating ranges (24), for the stepwise (31) and piecewise linear (33)–(34) approximation models (with tighter bounds for risk-averse strategies). This is also apparent in the (ex-ante) expected operating profit in the day-ahead scheduling problem (prior to the out-of-sample evaluation): for the same risk-attitude ε, the piecewise linear

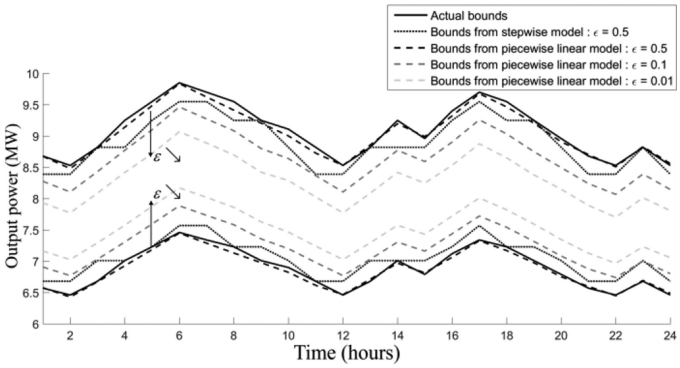

Fig. 7. Evolution of the safe operating zone in pump mode over time.

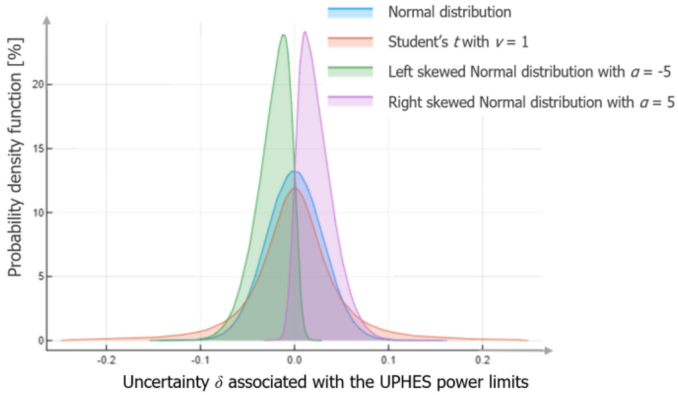

Fig. 8. Distributions of uncertainties used in the out-of-sample analysis.

approximation consistently yields higher profits. The highest (ex-ante) expected profits are – as expected – observed in the risk-neutral case ($\varepsilon = 0.5$). However, the (ex-post) out-of-sample violation probability of this (risky) deterministic solution is very high, with a reliability of 68.1% in the model using the piecewise linear approximation. As a result, one observes high real-time penalties and lower expected profits, leading to ex-post disappointment when the actual outcome is revealed. Low ε values (lower than 0.1) have a limited impact on real-time infeasibilities (i.e., high reliability of the operating schedule, hence, low imbalance fees), whereas the reliability strongly decreases with more risky approaches, as expected. This highlights the need for probabilistic approaches to avoid infeasibilities.

Third, all risk-aware solutions lead to much lower violation probabilities than their deterministic (risk-neutral) equivalent. In this way, the optimal risk-attitude improves on the deterministic solution by respectively 3.1% and 10.7% in terms of profits in the stepwise and piecewise linear formulations. Indeed, risky approaches (at high ε values) overestimate the expected profit and may generate losses in real time due to the low reliability (less than 85%) of the operating schedule. Conversely, when the UPHES operator becomes strongly risk-averse ($\varepsilon \to 0$), the benefits are more stable (i.e., low variation between scenarios), but this comes at the expense of the average performance of the strategy. Indeed, such policies excessively restrict the flexibility potential of UPHES systems, leading to less profitable schedules. For $\varepsilon \leq 0.01$, the UPHES operator does not provide operating reserves (thereby decreasing its economic value). In this case, the problem boils down to arbitrage in day-ahead market, which significantly reduces the computation time. Hence, it is possible to determine an optimal risk policy ε, characterized by the tradeoff between the revenues from offering operating reserves and the financial penalties arising from portfolio imbalances. By lowering its participation in operating reserve markets, a risk-averse UPHES operator is able to provide the regulation power in most reserve activation scenarios, avoiding imbalance penalties. Moreover, the lower revenues of the operating reserve markets is partly compensated by more revenue from the day-ahead market. In this case study, the optimal risk-awareness is $\varepsilon = 0.1$ for both the stepwise model and the piecewise linear approximation.

Fourth, in presence of model uncertainties, the conservativeness of the stepwise approximation (Fig. 7) works to its advantage for large ε-values, as illustrated by the high reliability and expected mean profit values. However, at optimal risk levels, the piecewise linear approximation results in higher profits (relative increase of 1.3%).

Fifth, except in (suboptimal) risk-averse strategies, the UPHES plant is operating (either in pump or turbine) across the whole scheduling horizon in order to provide spinning reserve since the unit cannot safely operate around 0 MW due to electromechanical constraints (Fig. 2). Since this requires scheduling the UPHES close to the boundaries of the safe operating range, a small error in the net head estimation may lead to the violation of the allowed output power range (and the associated imbalance payments) in case of full activation of operating reserves.

C. Robustness of the Results to the Assumption of Gaussian Uncertainties

In the proposed chance-constrained model, it is assumed that the net head uncertainty (which is converted into uncertain operating ranges) follows a Gaussian distribution with zero mean and $\sigma_{\text{opt}} = 0.025$ (reference case) [12]. It is thus important to evaluate the robustness of the solution obtained at the end of the optimization (in which the Gaussian assumption is used) against possible deviations from normality.

The quality of the risk-optimal solution obtained with the piecewise linear model ($\varepsilon = 0.1$) is tested through an out-of-sample analysis, in which the UPHES state is characterized by different distributions, depicted in Fig. 8 [47]: a normal distribution with zero mean and standard deviation of 0.03 (higher than σ_{opt}), a Student's *t* distribution with $\nu = 1$ degrees of freedom, as well as left- and right-skewed Normal distributions (where the skewness is controlled by the parameter α). The results are summarized in Table III.

Even if the uncertainty does not strictly follow normality, the reliability of the operating schedule deviates at most by 7.2 percentage points. Nonetheless, the results suggest that the standard deviation of the uncertain distribution is an important factor, since this parameter regulates the occurrence and probability of extreme scenarios (which may impact the solution reliability).

TABLE III
ROBUSTNESS OF THE OPTIMAL CHANCE-CONSTRAINED SOLUTION WITH RESPECT TO DIFFERENT REALIZATIONS OF UNCERTAINTIES

Distributions	Reliability [%]	Mean Profit [€]	Mean RT penalties [€]
Normal with $\sigma = 0.025$ (reference case)	85.9	1944.3	217.9
Normal with $\sigma = 0.03$	85.0	1886.1	276.0
Student's t with $\nu = 1$	83.2	1767.4	384.7
Left skewed Normal	78.7	1709.9	452.2
Right skewed Normal	91.5	2084.7	77.4

Indeed, both the Gaussian distribution with $\sigma = 0.03$, and the heavy tailed Student's *t* distribution have more values (compared to the reference case) far from the mean, which results in lower reliability and profit values.

As expected, the left-skewed ($\alpha = -5$) distribution decreases the reliability of the solution. Indeed, this function generates samples characterized by a smaller surface of the lower reservoir, which exacerbates head variations (and thus the safe operating range). Conversely, the right-skewed ($\alpha = 5$) distribution yields better performance than the reference case since the samples are associated with lower head variations, thereby reducing the risk of infeasibilities.

In general, in case the uncertainties are not strictly Gaussian, the proposed model is a convex approximation of the exact chance constrained optimization, which is useful to maintain the calculation burden within acceptable limits. In these cases, it is important that ε is interpreted as a guideline (approximated value) for risk-attitude, rather than a hard limit [47], since the model cannot guarantee the resulting out-of-sample reliability. If the parameters of the distribution are also uncertain, the proposed framework can be made more conservative using distributionally robust chance constrained programming [48].

V. CONCLUSION

In this paper, we propose a methodology to robustify the day-ahead scheduling problem faced by UPHES owners against both approximation errors and endogenous model uncertainties using chance constrained programming. The anticipation of the operator on the exogenous uncertainties (such as market outcomes) is modeled via scenarios, thereby combining the strengths of chance-constrained and scenario-based stochastic optimization. This resulting formulation is computationally efficient, and allows hedging against infeasible operating schedules (due to violations of the safe operating zones) while maximizing expected operating profits. In this paper, two different representations of these safe zones have been proposed and compared.

In a case study considering a hypothetical UPHES on an actual candidate site, it has been shown that an optimal risk-attitude ε may be determined to fully leverage the potential of the proposed framework, thereby outperforming both risk-neutral and risk-averse policies. Storage operators must thus strive for an accurate model of their hydraulic machine combined with chance constrains to manage the risk of infeasible operating conditions rather than relying on a conservative representation of the system's flexibility.

The proposed approach may be used by any operator that aims to immunize its scheduling procedure against endogenous model uncertainties and approximations in the models describing the flexibility of his assets. However, as an interesting perspective, the uncertainty on reserve capacity prices can also be integrated into the model, to better take into account the uncertainty associated with this market outcome.

REFERENCES

[1] A. van Stiphout, K. D. Vos, and G. Deconinck, "The impact of operating reserves on investment planning of renewable power systems," *IEEE Trans. Power Syst.*, vol. 32, no. 1, pp. 378–388, Jan. 2017.

[2] L. V. L. Abreu, M. E. Khodayar, M. Shahidehpour, and L. Wu, "Risk-constrained coordination of cascaded hydro units with variable wind power generation," *IEEE Trans. Sustain. Energy*, vol. 3, no. 3, pp. 359–368, Jul. 2012.

[3] A. A. S. de la Nieta, J. Contreras, and J. I. Muñoz, "Optimal coordinated wind-hydro bidding strategies in day-ahead markets," *IEEE Trans. Power Syst.*, vol. 28, no. 2, pp. 798–809, May 2013.

[4] E. Barbour, I. G. Wilson, J. Radcliffe, Y. Ding, and Y. Li, "A review of pumped hydro energy storage development in significant international electricity markets," *Renewable Sustain. Energy Rev.*, vol. 31, no. 61, pp. 421–32, Aug. 2016.

[5] T. Mercier, J. Jomaux, E. De Jaeger, and M. Olivier, "Provision of primary frequency control with variable-speed pumped-storage hydropower," in *Proc. IEEE Powertech*, 2017, pp. 1–6.

[6] R. Alvarado, A. Niemann, and T. Wortberg, "Underground pumped-storage hydroelectricity using existing coal mining infrastructure," in *Proc. 36th IAHR World Congr.*, 2015.

[7] A. Poulain, J.-R. de Dreuzy, and P. Goderniaux, "Pump hydro energy storage systems (PHES) in groundwater flooded quarries," *J. Hydrol.*, vol. 559, pp. 1002–1012, 2018.

[8] E. Pujades, P. Orban, S. Bodeux, P. Archambeau, S. Erpicum, and A. Dassargues, "Underground pumped storage hydropower plants using open pit mines: How do groundwater exchanges influence the efficiency?" *Appl. Energy*, vol. 190, pp. 135–146, 2017.

[9] C. I. Lee and J. J. Song, "Rock engineering in underground energy storage in Korea," *Tunnelling Underground Space Technol.*, vol. 18, no. 5, pp. 467–483, 2003.

[10] M. J. Severson, "Preliminary evaluation of establishing an underground taconite mine, to be used later as a lower reservoir in pumped hydro storage facility, on the Mesabi Iron Range, Minnesota," Nat. Resources Res. Inst., Univ. Minesota, Duluth, MN, USA, Tech. Rep. NRRI/RI-2011/02, 2011.

[11] E. Pujades *et al.*, "Hydrochemical changes induced by underground pumped storage hydropower and their associated impacts," *J. Hydrol.*, vol. 563, pp. 927–941, 2018.

[12] Smart Water Project, "Pumped hydro storage, outcomes and perspectives," in *Proc. Cluster TWEED Conf.*, May 2018, p. 2.

[13] G. Steeger, L. A. Barroso, and S. Rebennack, "Optimal bidding strategies for hydro-electric producers: A literature survey," *IEEE Trans. Power Syst.*, vol. 29, no. 4, pp. 1758–1766, Jul. 2014.

[14] J. I. Pérez-Diaz, M. Chazarra, J. Garcia-Gonzalez, G. Cavazzini, and A. Stoppato, "Trends and challenges in the operation of pumped-storage hydropower plants," *Renewable Sustain. Energy Rev.*, vol. 44, pp. 767–784, 2015.

[15] R. Taktak and C. D'Ambrosio, "An overview on mathematical programming approaches for the deterministic unit commitment problem in hydro valleys," *Energy Syst.*, vol. 8, no. 1, pp. 57–79, 2017.

[16] J. S. Yang and N. Chen, "Short term hydrothermal coordination using multi-pass dynamic programming," *IEEE Trans. Power Syst.*, vol. 4, no. 3, pp. 1050–1056, Aug. 1989.

[17] A. Arce, T. Ohishi, and S. Soares, "Optimal dispatch of generating units of the Itaipu hydroelectric plant," *IEEE Trans. Power Syst.*, vol. 17, no. 1, pp. 154–158, Feb. 2002.

[18] J. P. S. Catalao, S. J. P. S. Mariano, V. M. F. Mendes, and L. A. F. M. Ferreira, "Scheduling of head-sensitive cascaded hydro systems: A nonlinear approach," *IEEE Trans. Power Syst.*, vol. 24, no. 1, pp. 337–346, Feb. 2009.

[19] A. J. Wood and B. F. Wollenberg, *Power Generation, Operation, and Control*. New York, NY, USA: Wiley, 1996.

[20] E. Ni, X. H. Guan, and R. Li, "Scheduling hydrothermal power systems with cascaded and head-dependent reservoirs," *IEEE Trans. Power Syst.*, vol. 14, no. 3, pp. 1127–1132, Aug. 1999.
[21] E. C. Finardi and E. L. da Silva, "Solving the hydro unit commitment problem via dual decomposition and sequential quadratic programming," *IEEE Trans. Power Syst.*, vol. 21, no. 2, pp. 835–844, May 2006.
[22] P. H. Chen and H. G. Hang, "Genetic aided scheduling of hydraulically coupled plants in hydro-thermal coordination," *IEEE Trans. Power Syst.*, vol. 11, no. 2, pp. 975–981, May 1996.
[23] R. Naresh and J. Sharma, "Hydro system scheduling using ANN approach," *IEEE Trans. Power Syst.*, vol. 15, no. 1, pp. 388–395, Feb. 2000.
[24] B. H. Yu, X. H. Yuan, and J. W. Wang, "Short-term hydro-thermal scheduling using particle swarm optimization method," *Energy Convers. Manage.*, vol. 48, no. 7, pp. 1902–1908, Jul. 2007.
[25] G. Chang *et al.*, "Experiences with mixed integer linear programming based approaches on short-term hydro scheduling," *IEEE Trans. Power Syst.*, vol. 16, no. 4, pp. 743–749, Nov. 2001.
[26] E. C. Finardi, F. Y. K. Takigawa, and B. H. Brito, "Assessing solution quality and computational performance in the hydro unit commitment problem considering different mathematical programming approaches," *Elect. Power Syst. Res.*, vol. 136, pp. 212–222, Jul. 2016.
[27] X. Guan, A. Svoboda, and C.-A. Li, "Scheduling hydro power systems with restricted operating zones and discharge ramping constraints," *IEEE Trans. Power Syst.*, vol. 14, no. 1, pp. 126–131, Feb. 1999.
[28] E. Xi, X. Guan, and R. Li, "Scheduling hydrothermal power systems with cascaded and head-dependent reservoirs," *IEEE Trans. Power Syst.*, vol. 14, no. 3, pp. 1127–1132, Aug. 1999.
[29] A. J. Conejo, J. M. Arroyo, J. Contreras, and F. A. Villamor, "Self-scheduling of a hydro producer in a pool-based electricity market," *IEEE Trans. Power Syst.*, vol. 17, no. 4, pp. 1265–1272, Nov. 2002.
[30] A. Borghetti, C. D'Ambrosio, A. Lodi, and S. Martello, "An MILP approach for short-term hydro scheduling and unit commitment with head-dependent reservoir," *IEEE Trans. Power Syst.*, vol. 23, no. 3, pp. 1115–1124, Aug. 2008.
[31] C. Cheng, J. Wang, and X. Wu, "Hydro unit commitment with a head-sensitive reservoir and multiple vibration zones using MILP," *IEEE Trans. Power Syst.*, vol. 31, no. 6, pp. 4842–4852, Nov. 2016.
[32] C. H. Chen, N. Chen, and P. B. Luh, "Head dependence of pump-storage-unit model applied to generation scheduling," *IEEE Trans. Power Syst.*, vol. 32, no. 4, pp. 2869–2877, Jul. 2017.
[33] G. E. Alvarez, M. G. Marcovecchio, and P. A. Aguirre, "Security-constrained unit commitment problem including thermal and pumped storage units: An MILP formulation by the application of linear approximations techniques," *Elect. Power Syst. Res.*, vol. 154, pp. 67–74, Jan. 2018.
[34] D. Apostolopoulou, Z. De Grève, and M. McCulloch, "Robust optimization for hydroelectric system operation under uncertainty," *IEEE Trans. Power Syst.*, vol. 33, no. 3, pp. 3337–3348, May 2018.
[35] A. L. Diniz and M. E. P. Maceira, "A four-dimensional model of hydro generation for the short-term hydrothermal dispatch problem considering head and spillage effects," *IEEE Trans. Power Syst.*, vol. 23, no. 3, pp. 1298–1308, Aug. 2008.
[36] B. Tong, Q. Zhai, and X. Guan, "An MILP based formulation for short term hydro generation scheduling with analysis of the linearization effects on solution feasibility," *IEEE Trans. Power Syst.*, vol. 28, no. 4, pp. 3588–3599, Nov. 2013.
[37] J.-F. Toubeau, J. Bottieau, F. Vallée, and Z. De Grève, "Improved day-ahead predictions of load and renewable generation by optimally exploiting multi-scale dependencies," in *Proc. 7th IEEE Conf. Innovative Smart Grid Technol.*, Dec. 2017, pp. 1–5
[38] J.-F. Toubeau, J. Bottieau, F. Vallée, and Z. De Grève, "Deep learning-based multivariate probabilistic forecasting for short-term scheduling in power markets," *IEEE Trans. Power Syst.*, vol. 34, no. 2, pp. 1203–1215, Mar. 2019.
[39] G. Ardizzon, G. Cavazzini, and G. Pavesi, "A new generation of small hydro and pumped-hydro power plants: Advances and future challenges," *Renewable Sustain. Energy Rev.*, vol. 31, pp. 746–761, 2014.
[40] V. Dvorkin, S. Delikaraoglou, and J. M. Morales, "Setting reserve requirements to approximate the efficiency of the stochastic dispatch," *IEEE Trans. Power Syst.*, vol. 34, no. 2, pp. 1524–1536, Mar. 2019.
[41] J.-F. Toubeau, Z. De Grève, and F. Vallée, "Medium-term multi-market optimization for virtual power plants: A stochastic-based decision environment," *IEEE Trans. Power Syst.*, vol. 33, no. 2, pp. 1399–1410, Mar. 2018.
[42] Commission Regulation (EU), "Establishing a guideline on electricity balancing," 2017.
[43] ENTSO-E, "Network code on load-frequency control and reserves," Brussels, Belgium, Tech. Rep., Feb. 2012.
[44] K. Bruninx, Y. Dvorkin, E. Delarue, H. Pandžić, W. D'haeseleer, and D. S. Kirschen, "Coupling pumped hydro energy storage with unit commitment," *IEEE Trans. Sustain. Energy*, vol. 7, no. 2, pp. 786–796, Apr. 2016.
[45] K. Bruninx, Y. Dvorkin, E. Delarue, W. D'haeseleer, and D. S. Kirschen, "Valuing demand response controllability via chance constrained programming," *IEEE Trans. Sustain. Energy*, vol. 9, no. 1, pp. 178–187, Jan. 2018.
[46] G. Hahn and S. Shapiro, *Statistical Models in Engineering*. New York, NY, USA: Wiley, 1967.
[47] L. A. Roald, "Optimization methods to manage uncertainty and risk in power systems operation," Doctoral Dissertation, ETH Zurich, Zürich, Switzerland, 2016.
[48] M. Lubin, Y. Dvorkin, and S. Backhaus, "A robust approach to chance constrained optimal power flow with renewable generation," *IEEE Trans. Power Syst.*, vol. 31, no. 5, pp. 3840–3849, Sep. 2016.

Jean-François Toubeau (M'18) was born in Mons, Belgium, in 1990. He received the degree in civil electrical engineering and the Ph.D. degree in electrical engineering from the University of Mons, Mons, Belgium, in 2013 and 2018, respectively. He is currently a Post-doctoral Researcher of the Belgian Fund for Research (F.R.S/FNRS) within the Electrical Power Engineering Unit of the same faculty. His research interests include decision-making in the context of power markets as well as data analytics.

Zacharie De Grève (M'12) received the Electrical and Electronics Engineering degree from the Faculty of Engineering of Mons, University of Mons, Mons, Belgium, in 2007, and the Ph.D. degree in electrical engineering from the University of Mons. He has been a Research Fellow of the Belgian Fund for Research (F.R.S/FNRS) until 2012. He is currently a Researcher with the Electrical Power Engineering Unit, University of Mons, and has been a part-time Lecturer since September 2019. He conducts transverse research in machine learning, optimization, and energy economics applied to modern electricity networks with a high share of renewables, in order to contribute to the energy transition.

Pascal Goderniaux received the Ph.D. degree in geological engineering from the University of Liège, Liège, Belgium. He is currently a Professor in hydrogeology with the Faculty of Engineering, University of Mons, Mons, Belgium. He has been a Research Fellow of the Belgian Fund for Research (F.R.S/FNRS) until 2010. He performed a postdoctoral research with University of Rennes 1 (France) from 2010 to 2012. His main research activities are related to general and applied hydrogeology, modeling of groundwater flow and solute transport in subsurface rock reservoirs, and geothermal exploitation.

François Vallée (M'09) received the degree in civil electrical engineering and the Ph.D. degree in electrical engineering from the Faculty of Engineering, University of Mons, Mons, Belgium, in 2003 and 2009, respectively. He is currently an Associate Professor with the Electrical Power Engineering Unit of the same faculty. He has authored or coauthored several publications in that field and the Ph.D. work has been awarded by the SRBE/KBVE Robert Sinave Award in 2010. His research interests include PV and wind generation modeling for electrical system reliability studies in the presence of dispersed generation. He is currently a member of the governing board from the "Société Royale Belge des Electriciens—SRBE/KBVE" in 2017 and is an Associate Editor for the *International Transactions on Electrical Energy Systems* (Wiley).

Kenneth Bruninx (M'16) received the M.Sc. degree in energy engineering and the Ph.D. degree in mechanical engineering from the University of Leuven (KU Leuven), Leuven, Belgium, in 2011 and 2016, respectively. He is currently a Post-doctoral Research Fellow of the Research Foundation – Flanders (FWO) with the University of Leuven Energy Institute, TME branch (energy conversion), VITO (the Flemish Institute for Technological Research), and EnergyVille, a joint venture of KU Leuven, VITO, and IMEC.